



# Temperature-dependent properties of electrochemically grown CdS thin films from acetate precursor

S. Z. Werta<sup>1</sup> · O. K. Echendu<sup>1</sup> · F. B. Dejene<sup>1</sup> · Z. N. Urgessa<sup>2</sup> · J. R. Botha<sup>2</sup>

Received: 5 June 2018 / Accepted: 21 July 2018 / Published online: 3 August 2018  
© Springer-Verlag GmbH Germany, part of Springer Nature 2018

## Abstract

Cadmium sulphide (CdS) thin films have been successfully deposited on glass/fluorine-doped tin oxide (glass/FTO) from an aqueous electrolyte solution containing cadmium acetate  $\text{Cd}(\text{CH}_3\text{COO})_2$  and sodium thiosulphate ( $\text{Na}_2\text{S}_2\text{O}_3$ ) using electrodeposition technique. The deposition electrolytic bath temperature was varied at 45, 65 and 85 °C. Two electrode system was applied and the corresponding structural, optical, morphological and compositional properties of these thin films have been characterized using X-ray diffraction, UV–Vis spectrophotometry, scanning electron spectroscopy, scanning probe microscopy and energy dispersive X-ray spectroscopy, respectively. The effect of post growth annealing on the structural, optical and morphological quality of the thin films is also reported. The results show that, growth temperature has significant influence on structural and optical properties of the film properties. Increasing the electrolytic solution temperature resulted in slight improvement in crystallinity of CdS thin films in both as deposited and annealed conditions. Due to increase in bath temperature from 45 to 85 °C the energy band gap narrows down from 2.45 to 2.38 eV for as deposited films and 2.42–2.22 eV for annealed films. The increase in deposition temperature improves the atomic ratio of Cd to S. Similarly, the grain sizes of the films increase with increase in growth temperature.

## 1 Introduction

Cadmium sulfide (CdS) is one of the most investigated thin film semiconductors for photovoltaic application in the last six decades [1–7]. CdS is a compound of group II and VI elements having a wide energy band gap of 2.42 eV and mostly used as n-type window material in CdS/CdTe, CdS/CuInSe and CdS/CuInGaSe solar cells [8–12]. The compound is used in other device applications such as in gas sensors, field effect transistors, optical filters, multilayer light emitting diodes and for optoelectronic devices. CdS thin film can be deposited using different methods including chemical bath deposition (CBD) [13, 14], electrodeposition [15, 16], molecular beam epitaxy (MBE) [17], metal organic chemical vapor deposition (MOCVD) [18], close space sublimation (CSS) [19], successive ionic layer adsorption and reaction (SILAR) [20], screen printing [21], Sol–gel [22],

RF sputtering [23], pulsed laser deposition (PLD) [24], and physical vapor deposition (PVD) [25].

Each method has its advantages and disadvantages in device applications. Among these methods electrodeposition methods is very interesting with many advantages such as use in large area deposition, easy process control, minimum waste generation and self-purification of electrolytes. It is observed that, in the deposition of CdS thin films using electrodeposition method, parameters such as concentration of ions in the deposition electrolyte, deposition time, stirring, pH, electrodes used and applied voltage play a vital role in the quality of the film produced [26]. If these parameters are optimized, efficient CdS thin film which can be applied for different applications will be produced.

Mainly, electrodeposited CdS (ED-CdS) thin films are grown using  $\text{CdCl}_2$ ,  $\text{CdSO}_4$  and  $\text{Cd}(\text{NO}_3)_2$  as cadmium precursors [7, 15, 16, 27]. Using these precursors cubic and hexagonal phases of ED-CdS thin film co-exists. But after annealing most commonly the cubic phase of the film diminishes or disappears completely. However, in chemical bath deposition method using cadmium acetate ( $\text{Cd}(\text{CH}_3\text{COO})_2$ ) precursor this phenomenon does not occur and cadmium acetate is known as a suitable precursor for chemical bath deposition. In addition, one of the challenges in

✉ S. Z. Werta  
solomonwerta@gmail.com

<sup>1</sup> Department of Physics, University of the Free State Qwa Qwa Campus, Phuthaditjhaba, South Africa

<sup>2</sup> Department of Physics, Nelson Mandela University, Port Elizabeth, South Africa

electrodeposition method is sulphur precipitation at elevated temperature. Comparing with  $\text{CdCl}_2$ , cadmium acetate bath has small precipitation. Hence, in this paper we investigate, the effect of electrolytic solution temperature on the structural, optical, morphological and compositional properties of electroplated CdS thin films using cadmium acetate  $\text{Cd}(\text{CH}_3\text{COO})_2$  as Cd source and which is not yet reported using electrodeposition method.

## 2 Experimental details

### 2.1 Deposition of the CdS films

CdS thin films were deposited using glass/FTO (glass/fluorine-doped tin oxide) substrate. The substrates used for the deposition of CdS thin films were  $2\text{ cm} \times 2.6\text{ cm}$  surface area each. Before the deposition was carried out, the substrates were immersed in de-ionised water with laboratory soap solution and cleaned ultrasonically for 30 min. Then the substrates were cleaned with de-ionized water and finally with ethanol, acetone, methanol, respectively, using de-ionized water to rinse in between washings, and then dried in air. The deposition electrolyte solution was prepared from 0.3 M of cadmium acetate ( $\text{Cd}(\text{CH}_3\text{COO})_2$ ) as cadmium source and 0.03 M sodium thiosulphate ( $\text{Na}_2\text{S}_2\text{O}_3 \cdot 5\text{H}_2\text{O}$ ) as sulphur source in a 400 ml of deionized water. Both chemicals are laboratory reagent grade purchased from Emsure, Germany with purity of 99.0%. The solution was stirred for 6 h at room temperature until chemicals dissolved well. To accomplish the electrodeposition of CdS thin films, the

glass/FTO substrate was attached to carbon plate using polytetrafluoroethylene (PTFE) which serves as working electrode. To determine the possible potential to grow CdS thin films, a cyclic voltammetry measurement was taken using a computerized Gill AC potentiostat (ACM Instruments, United Kingdom) in two-electrode configuration, with a clean fluorine-doped tin oxide-coated glass (glass/FTO) as the working electrode and a high-purity graphite rod as the counter electrode. From the resulting voltammogram, the possible deposition voltage for CdS thin films was determined to be in between 1350 and 1500 mV as shown in Fig. 1. Taking these possible cathodic potentials, different preliminary depositions were made on different FTO substrates to optimize the potential. Finally, the best deposition voltage was settled at 1450 mV. The electrolytic solution pH was maintained at  $1.8 \pm 0.02$  and dilute sulphuric acid ( $\text{H}_2\text{SO}_4$ ) and ammonium hydroxide ( $\text{NH}_4\text{OH}$ ) were used to control the pH. Moderate stirring rate of electrolytic bath and 30 min deposition time were applied.

The deposition of CdS thin films was carried out at three different temperatures: 45, 65 and 85 °C. Three pre-cleaned glass/FTO substrates were prepared to carry out the deposition process of CdS thin films. When the temperature reached at deposition temperature of interest, the FTO substrate was immersed in the electrolytic solution for 30 min deposition time with moderate stirring, and a deposition potential of 1450 mV applied. After deposition, the samples were removed from the solution and rinsed with deionized water and then dried in air. Finally, each CdS thin film sample was cut in to two equal pieces. One-half is designated as deposited sample and the other annealed for 10 min at

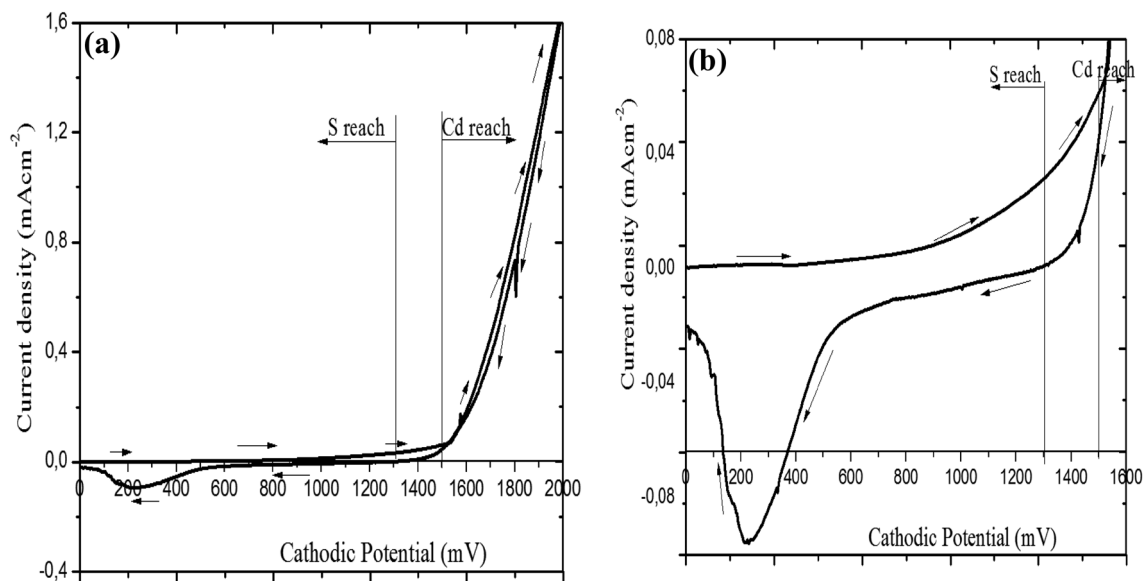


**Fig. 1** **a** Two-electrode cyclic voltammogram of CdS deposition electrolyte bath with an aqueous solution of 0.3 M  $\text{Cd}(\text{CH}_3\text{COO})_2$  and 0.03 M  $\text{Na}_2\text{S}_2\text{O}_3 \cdot 5\text{H}_2\text{O}$  and **b** Expanded view showing the CdS deposition potential range

400 °C to investigate the effect of annealing. The as-deposited ED-CdS thin films at low temperature were greenish yellow in colour but as the deposition temperature increases to 65 °C the colour changed to bright yellow and then dark greenish yellow at 85 °C.

After annealing, uniformity of the resulting CdS improved and the physical appearance of these films changed. At 45 °C the appearance of the ED-CdS film looks greenish yellow almost similar with as-deposited sample. Beside this sample grown at 45 °C other ED-CdS thin films grown at 65 and 85 °C come to orange yellow colour.

X-ray diffraction (XRD) patterns were recorded to characterize the structure of the CdS thin films using Bruker D 8 X-ray diffractometer with a wavelength of 1.54 Å. Optical transmission and absorbance data were obtained with a Shimadzu UV-1700PC spectrophotometer. Scanning electron microscopy (SEM) was used to analyse the surface morphologies of the samples and scanning probe microscopy to study the surface roughness of the samples. Energy dispersive X-ray spectroscopy (EDX) was used to determine the chemical composition of the films.

### 3 Results and discussion

#### 3.1 Structural properties

CdS thin film can grow in cubic, hexagonal, orthorhombic or mixed phase depending on deposition conditions [5, 6, 28]. According to the results presented in Fig. 2a cubic and

hexagonal structure were observed for as-deposited conditions and after annealing only cubic structure was observed. These XRD peaks agree with others previous reports [29–31]. It is observed that there is a slight improvement in crystallinity with increase in temperature of the electrolytic solution and annealing of the grown samples [32, 33]. The identified diffraction peaks match those of Joint Committee on Powder Diffraction and Standards (JCPDS) reference files 01-075-0581 for cubic CdS and 01-075-1545 for hexagonal CdS.

As can be seen from the XRD patterns of as-deposited sample at 45 °C (Fig. 2a) there is appearance of small XRD peaks at  $2\theta = 26.55$ , 28.53 and 45.8 corresponding to diffractions from (111)C, (101)H and (220)C crystal planes respectively. When the temperature was 65 °C the sample shows diffraction peaks at  $2\theta = 26.50$ , 45.78 and 47.78 corresponding to (111)C, (220)C and (103)H diffraction planes respectively. Samples grown at 85 °C growth temperature show a slight increase in peaks intensity and the peaks were at  $2\theta = 26.5$ , 30.69 and 43.91 corresponding to (111)C, (200)C and (220)C diffraction planes respectively.

After annealing, due to the fact that only very thin CdS is formed on the substrate, the sample grown at 45 °C, shows no observable peak. At a temperature of 65 °C there exist one peaks that coincides with the FTO peak at angle of  $2\theta = 26.5$  corresponding to the (111)C. But as the electrolytic bath temperature increases more (to 85 °C) there is a slight improvement in the peaks with two peaks emerging at angles of  $2\theta = 26.5$  and 44.04 and corresponding to (111)C and (220)C of CdS. CdS thin films

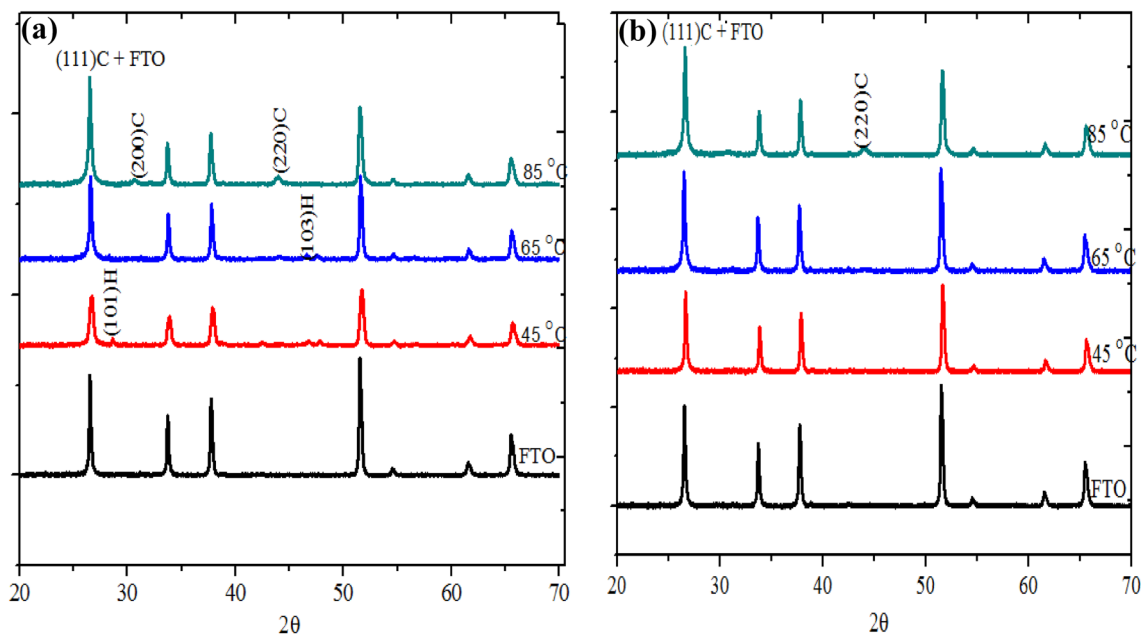


**Fig. 2** XRD patterns of CdS thin films grown at 45, 65 and 85 °C in a as deposited (b) annealed forms

grown by electrodeposition method using CdCl<sub>2</sub> precursor have been reported to have more visible and clearly defined XRD peaks than those grown with Cd(CH<sub>3</sub>COO)<sub>2</sub> precursor [7, 8, 15, 16].

Table 1 summarizes the structural parameters obtained for these films.

According to the Scherrer formula, the crystalline size of a thin film can be determined as [34]:

$$D = \frac{K\lambda}{\beta \cos \theta} \tag{1}$$

where *D* is the mean size of the crystallites, *K* is the Scherrer constant (0.94), *β* is the broadening of the diffraction line measured at half of its maximum intensity in radian, *λ* is the wavelength of the X-ray used (1.54 Å) and *θ* is the diffraction angle.

### 3.2 Optical properties

UV–Vis spectroscopy helps us to study optical properties of materials. The optical properties of CdS thin films were determined from absorbance and transmittance measurements in the range of 200–1000 nm. Both Figs. 3 and 4, respectively, show absorbance and transmittance graphs of CdS thin films, respectively, for both as-deposited and annealed samples. Figure 3a, b clearly shows that electrolytic bath solution temperature significantly affects the absorbance of CdS thin film. The increase in electrolytic bath temperature increases the absorbance of CdS thin films. As temperature increases the absorption graph becomes steeper. Some physical effects such as structural, morphology (surface roughness) and defect density, apart from thickness, may affect the absorbance of ED-CdS thin film. Annealing can play a significant role in adjusting such physical factors which eventually affect the absorbance of CdS films.

**Table 1** Diffraction angle, d-spacing and *h k l* values extracted from XRD measurement for both as deposited and annealed CdS thin films

Temperature (°C)	As-deposited					Annealed				
	2θ (°)	<i>h k l</i>	d-spacing (Å)	β (°)	<i>D</i> (nm)	2θ (°)	<i>h k l</i>	d-spacing (Å)	β (°)	<i>D</i> (nm)
45	26.70	(111)	3.35	0.39	21.5	26.62	(111)	3.34	0.27	31.6
	28.63	(101)	3.12	0.18	40.9	–	–	–	–	–
	45.79	(220)	1.96	0.41	21.7	–	–	–	–	–
65	26.50	(111)	3.36	0.22	38.0	26.50	(111)	3.38	0.30	37.9
	45.78	(200)	1.96	0.41	19.9	43.79	(220)	2.06	0.60	12.3
	47.78	(103)	1.91	0.34	24.6	–	–	–	–	–
85	26.50	(111)	3.36	0.24	34.9	26.56	(111)	3.36	0.25	32.2
	30.61	(200)	2.92	0.48	17.4	–	–	–	–	–
	43.95	(220)	2.06	0.55	14.9	44.04	(220)	2.06	0.42	13.9

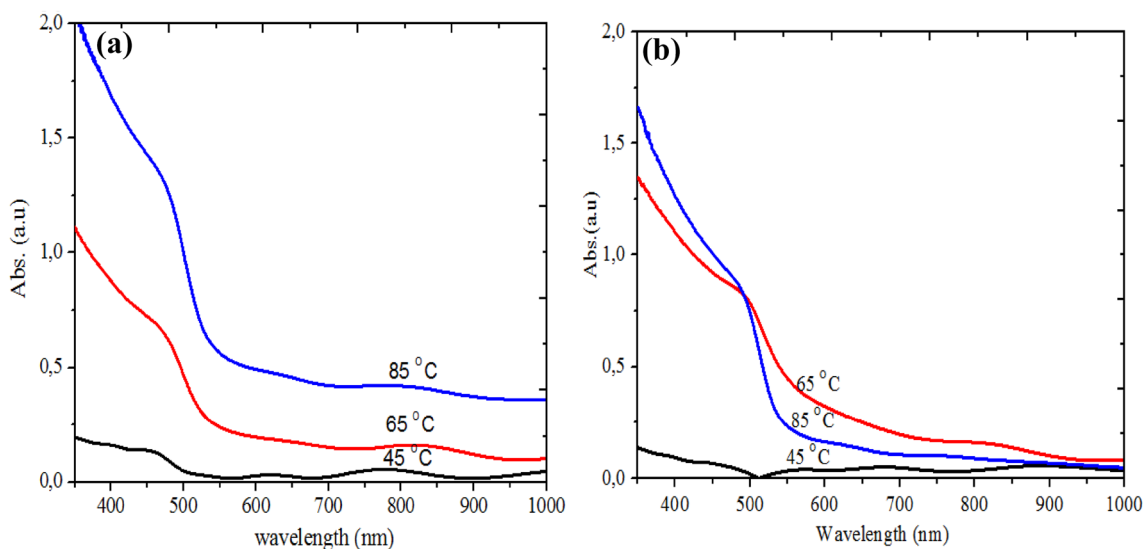


**Fig. 3** Absorbance of CdS thin films as a function of bath temperature for **a** as deposited and **b** annealed samples

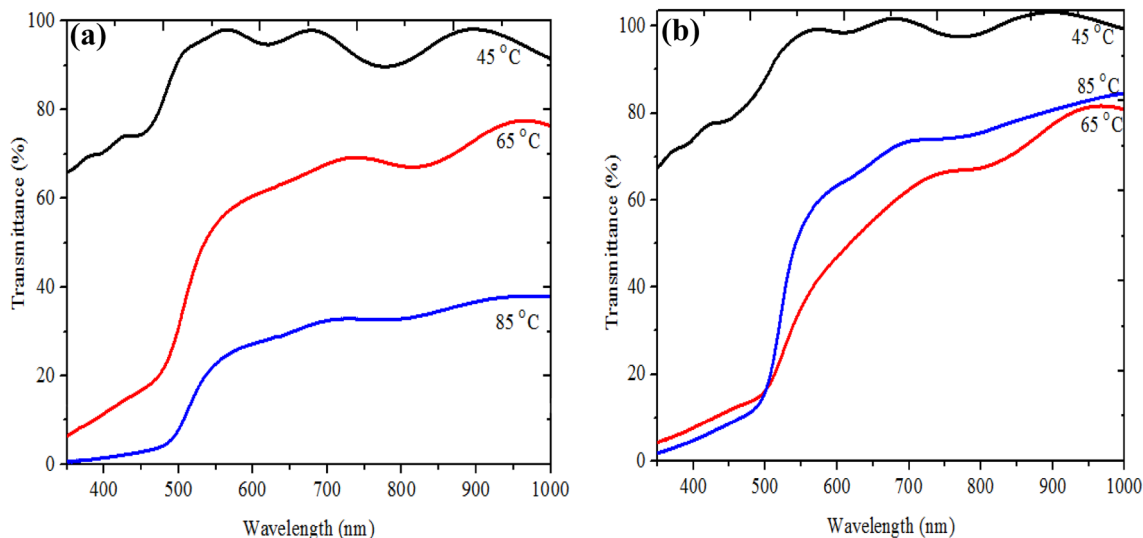


**Fig. 4** Transmittance of CdS thin films as a function of wave length for **a** as deposited and **b** annealed samples

Figure 4a, b, shows the transmittance graph of as-deposited and annealed condition of ED-CdS thin film. At low growth temperature (45 °C), due to the fact that production of Cd<sup>2+</sup> and S<sup>2-</sup> ions is low, the ED-CdS thin film is expected to be thin in thickness and this results in high transmittance values. As the electrolytic bath temperature increases to 65 and 85 °C the transmittance value gradually decreased. The transmission of the light through the material depends upon the film thickness. Increase in the temperature increases the formation of CdS material which leads to increase in film thickness. Absorbance and transmittance are mostly associated with thickness of the

sample. It is obvious that thicker films absorb more light that results in low transmittance and vice versa. After annealing for similar reasons given for the absorbance graph above, there is an improvement in transmittance value at all three electrolytic bath temperatures and the highest transmittance values are recorded at 45 °C. But at low temperature the stoichiometry of CdS thin film is poor. So to resolve such issue it is recommended to grow at high electrolytic bath temperature by reducing deposition time. Generally, from the absorbance and transmittance graphs there is a decrease in transmittance for all films

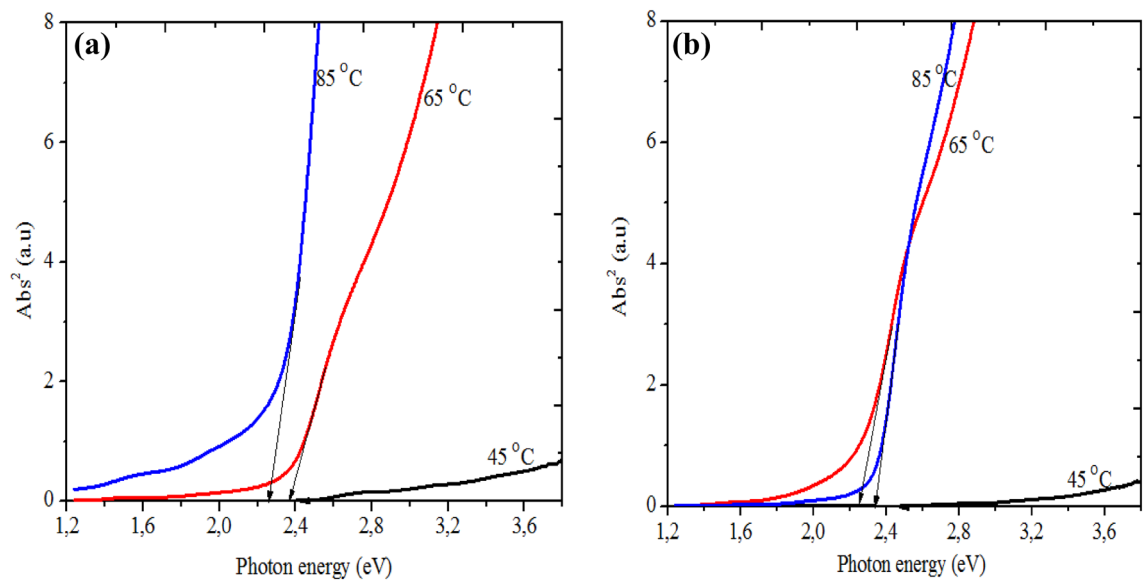


**Fig. 5** Graph of Abs<sup>2</sup> versus photon energy for **a** as-deposited and **b** annealed films grown at different temperatures

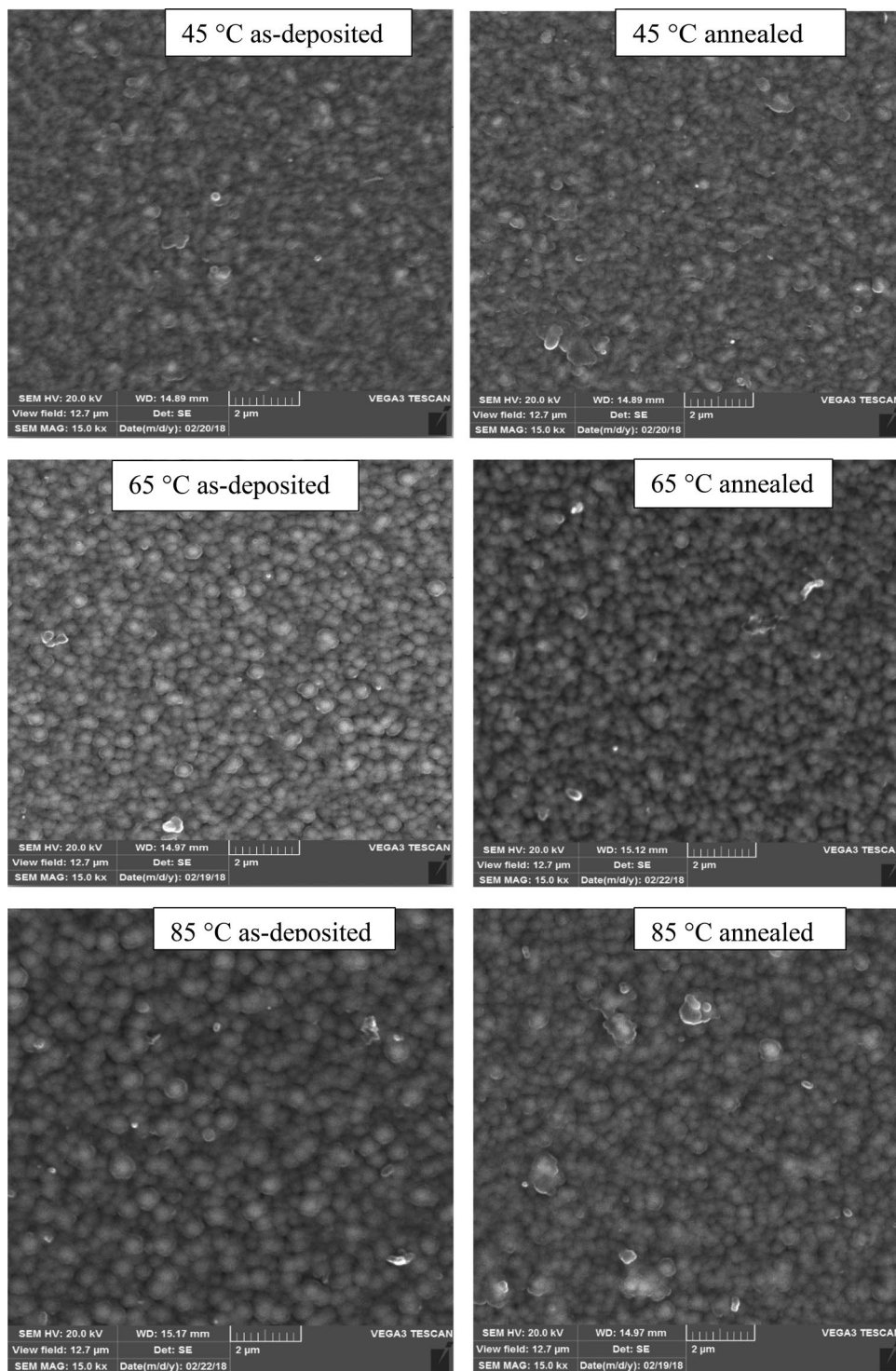


with increase in temperature; however, the high absorbance is related to the increase of film thickness.

Square of absorbance ( $Abs^2$ ) versus photon energy (eV) graph (Fig. 5a, b) has been used for the determination of optical band gap ( $E_g$ ) by extrapolation of the straight line

portion of the graph to zero  $Abs^2$ . It is observed that at 45 °C the energy band gap of CdS thin film for as deposited film was 2.45 eV. The increase in electrolytic bath temperature results in the band gap reduction to 2.4 and 2.38 for 65 and 85 °C temperature, respectively.

**Fig. 6** The SEM images of CdS films deposited under three electrolytic bath temperatures



When annealed the films energy band gap comes to 2.42–2.20 eV. The observed trend in the band gap arises, in the first place, because band gap is known to depend on film thickness in most cases. In case, the film with least thickness (film grown at 45 °C) shows the highest band gap and the film with highest thickness (that grown 85 °C) shows lowest band gap. In the case of annealing, re-crystallization occurs to produce better and more stable material. In the process, excess un-reacted species such as S and Cd may be lost, which may lead to either increase or decrease in band gap depending on the material involved and amount of atoms lost. The re-crystallisation process can also results in rearrangement of the crystalline and grains in the material in such a way as to increase photon absorption or even scattering which results reduce band gap.

### 3.3 Scanning electron microscopy (SEM)

Scanning electron microscopy (SEM) technique was used to study the morphology of CdS thin films deposited at three different electrolytic bath temperatures. Figure 6 shows the surface morphology of the films. The obtained scanning electron microscopy images of ED-CdS thin film layers revealed that, at low temperature (45 °C), due to the fact that the film is sulphur- rich with small thickness, there is less compacted grains observed for both as-deposited and annealed conditions. While, as deposition temperature increases to 65 °C and then to 85 °C, well compacted (i.e with less gaps between grains) and well defined grains of CdS thin film were observed. In both conditions at 65 and 85 °C bath temperatures, the surface of ED-CdS thin film is covered better with larger well defined grains which are well packed together. This suggests that, increase in electrolytic bath temperature improves the morphology of ED-CdS thin film. The estimated grain sizes of as-deposited CdS thin film samples are in the range of 388–574 nm under the different temperature conditions. These large grain sizes result due to the agglomeration of small grains.

During annealing there is a significant change, improving the grain size of the samples and the estimated grain size of the annealed CdS thin films is in the range of 420–644 nm. This increase in grain size may be attributed to the annealing condition used which led to coalescence of small grains into large ones [32]. However, larger grain size is recommended for solar cell device because of having less grain boundaries and ease of electron movement with less scattering [16]. Generally, in both as-deposited and annealed conditions, when the growth temperature increases the grain size also increases significantly. Apart from the increase in grain size after annealing, the SEM images of the as-deposited and annealed samples look very much similar. This shows that the annealing condition did not degrade the surface

morphology of the films indicating the good uniformity of the films produced by electrodeposition as well as moderate annealing conditions. Figure 7 summarizes the variation of grain size with electrolytic bath temperature.

### 3.4 Scanning probe microscopy (SPM)

Scanning probe microscopy measurement technique was applied to investigate the surface roughness of ED-CdS thin films. For solar cell or any other engineering applications, measurement or study of surface nature of material is an important issue [35, 36].

SEM image tells us only the shape and magnitude (grain size) of cross-section of the top of the grains. The magnitudes of the surface roughness are quantitatively verified by comparing the root mean square (rms)-roughness value which can be obtained from SPM images shown in Fig. 8. Root mean square roughness is estimated from SPM using Eq. 2 [36].

$$R_q = \sqrt{\frac{1}{L} \int_0^L Z^2(x) dx} \quad (2)$$

where  $R_q$  is root mean square surface roughness,  $Z(x)$  is the function that describes the surface profile analyzed in terms of height ( $Z$ ) and position ( $x$ ) of the sample over the evaluation length ( $L$ ).

The root mean square surface roughness ( $R_q$ ) has been estimated in the range of 1.9–2.6 nm for as deposited films and 0.66–2.5 nm for annealed films of the ED-CdS thin films. As confirmed by the SPM images, due to the reason that at low temperature (45 °C) the deposition rate is lower and less amount of CdS is formed on the substrate, the highest surface roughness ( $R_q$ ) value of 2.6 nm

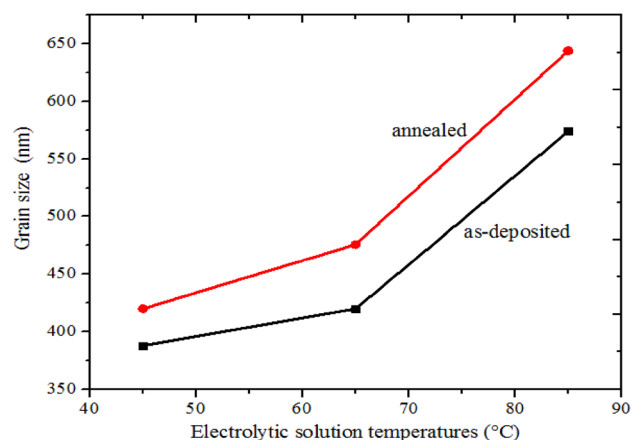
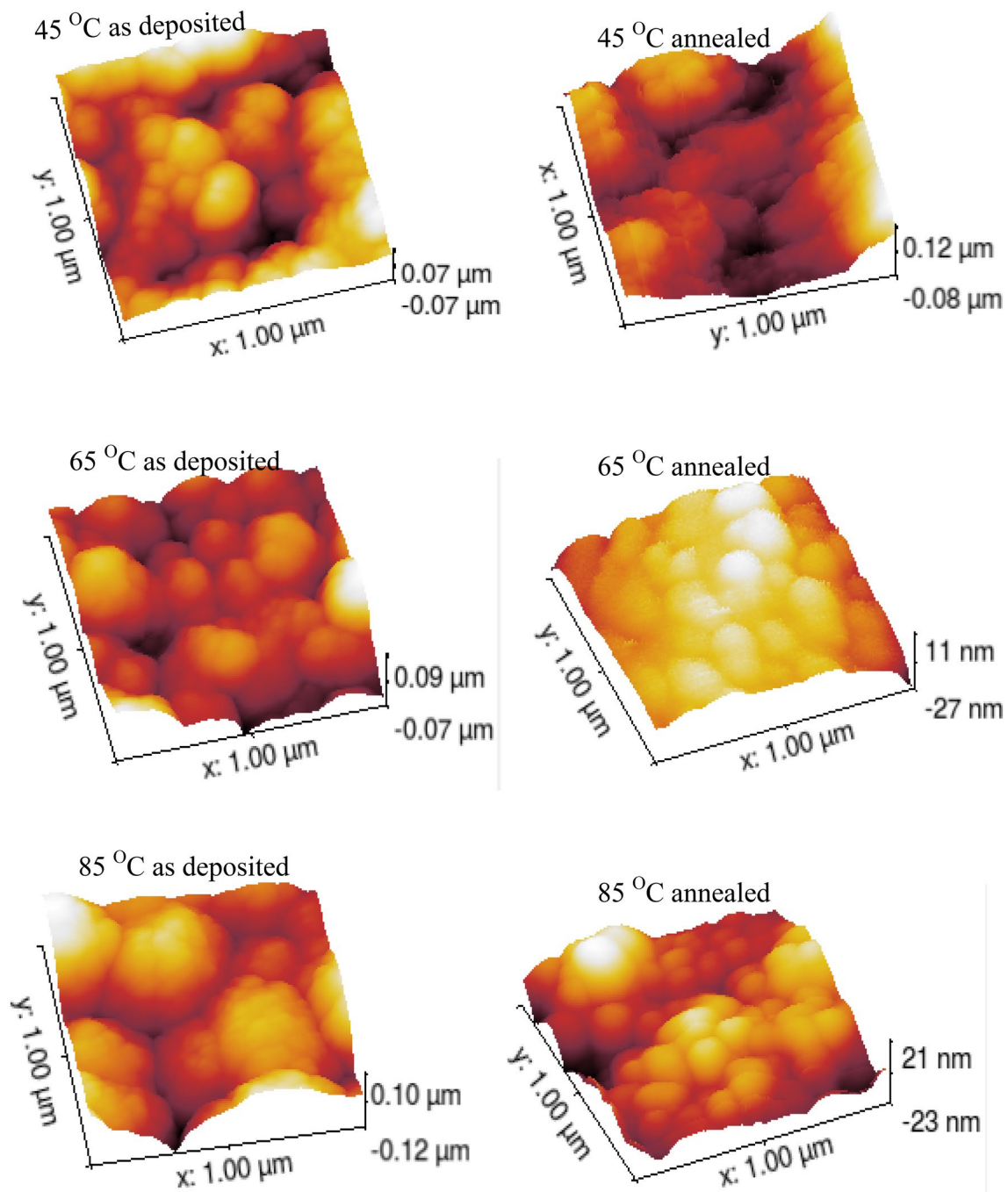


Fig. 7 Graph of grain size versus electrolytic bath temperature



**Fig. 8** The SPM images of CdS films deposited at three electrolytic bath temperatures

was measured for as-deposited conditions. This implies that the distances between CdS grains are far apart. After annealing CdS thin films have larger grain size due to the coalescence of small grains. These agglomerated of small grains minimize the distances between grains. For this reason, there is a slight improvement in minimizing roughness at 45 °C and significant improvement in minimizing

roughness at 65 and 85 °C. After annealing the highest roughness was observed for the film grown at 45 °C with a value of 2.5 nm. In both as deposited and annealed conditions as temperature increases as well as after annealed there is a decrease in the surface roughness of ED-CdS thin films. Figure 9 summarizes root mean square roughness versus electrolytic bath temperature.



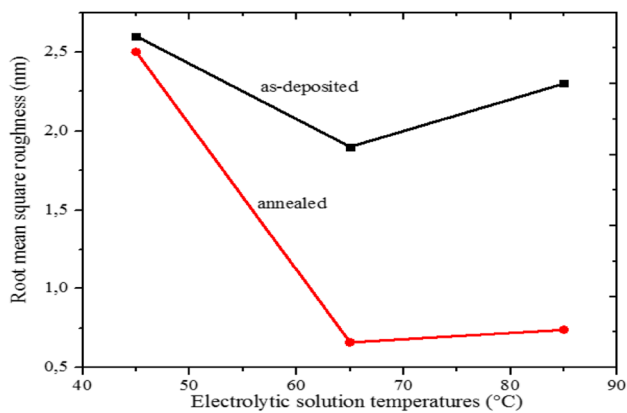


**Fig. 9** Graph of root mean square surface roughness versus electrolytic bath temperature

### 3.5 Compositional characterization

The EDX measurement has been used to confirm the composition of CdS thin films grown at three different temperatures. To save journal pages, Fig. 10 shows the spectra of both as-deposited and annealed CdS thin film grown at 85 °C since EDX spectra of all samples grown at the different temperatures are similar. From the spectrum it is observed that both Cd and S exist in the films. The peaks belonging to Sn, O and Si come from the glass/FTO substrate. In addition, carbon peak comes from carbon coating used in sample preparation from the measurement. Table 2 shows that, at low temperature (45 °C), due to the fact that sulphur deposits first there is more

sulphur in the CdS thin film than Cd. This results in 0.79 Cd/S ratio for the as deposited film and 0.69 for annealed film at this temperature. When the electrolytic bath temperature increases to 65 and 85 °C the formation of more stoichiometric CdS film is obtained. This implies that more Cd atoms are incorporated in the film as the electrolytic bath temperature increases. If one looks at the sample grown at 85 °C the ratio of Cd to S shows an improvement which is 0.87 as-deposited form and 0.86 in annealed forms [34, 37, 38].

Film thicknesses were estimated using Faraday’s Eq. (3). The estimated thicknesses of all films at these three temperatures are in the range of 176 to 543 nm and are summarized in Table 2.

$$L = \frac{1}{nFA} \frac{ItM}{d} \tag{3}$$

where  $L$  is the film thickness,  $F$  is Faraday’s constant,  $A$  is the area of the thin film,  $I$  is the deposition current,  $t$  is the deposition time,  $M$  is the molar mass of CdS,  $d$  is the density of CdS, and  $n$  is the number of electrons transferred in the reaction for the formation of 1 mol of CdS.

### 4 Conclusion

CdS thin films have been electrodeposited successfully on glass/FTO substrates at different temperatures using cadmium acetate and sodium thiosulphate as precursors. Results of structural, optical, morphological and compositional characterization reveal that CdS thin film grown at 85 °C shows

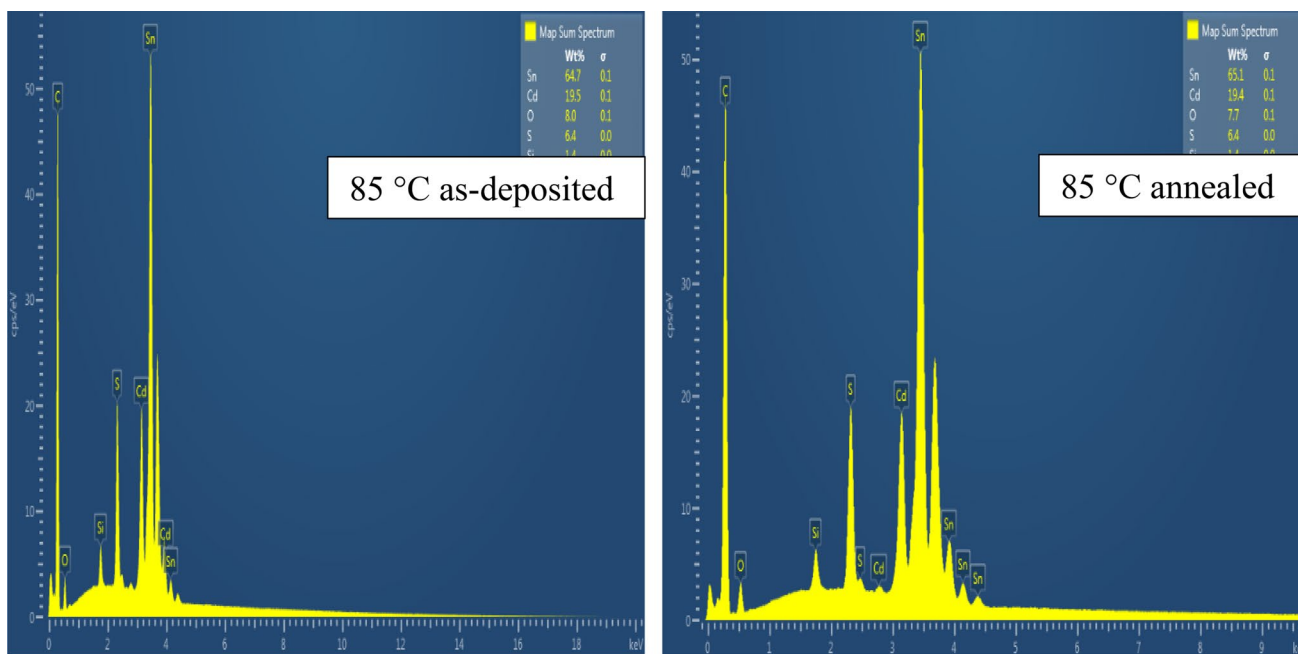


**Fig. 10** EDX spectra of the CdS thin films grown at 85°C

**Table 2** Atomic composition of CdS thin films grown at different temperatures

Temperature (°C)	Element	As deposited		Annealed		Thickness (nm)
		(%)	Ratio (Cd/S)	(%)	Ratio (Cd/S)	
45	Cd	44.1	0.79	40.8	0.69	176
	S	55.9		59.2		
65	Cd	46.4	0.86	46.4	0.87	334
	S	53.6		53.4		
85	Cd	46.5	0.87	46.4	0.86	543
	S	53.5		53.6		

better material properties compared to those grown at 45 and 65 °C. These result show that electrodeposited CdS thin films grown at high temperature (85 °C) have better quality for solar cell and other devices, thus underlining the impact of elevated growth temperature on quality of electrodeposited semiconductors for device application. Further work will focus on studying the electrical properties of these films and subsequently applying them in thin films solar cell fabrication as window or buffer materials.

**Acknowledgements** The authors would like to thank the University of the Free State, Research Directorate and the National Research Foundation, South Africa for funding the research that led to this paper.

### Compliance with ethical standards

**Conflict of interest** Authors declare no conflict of interest.

### References

1. A.G. Stanley, Massachusetts inst of tech Lexington Lincoln lab, (1967)
2. F.A. Shirland, *Adv. Energy Convers.* **6**, 201–221 (1966)
3. R.R. Arya, T. Warminski, R. Beaulieu, M. Kwietniak, J.J. Loferski, W. Giriat, *Sol. Energy Mater.* **8**, 471–481 (1983)
4. S. Dennison, *Electrochimica Acta* **38**, 2395–2403 (1993)
5. A. Ashour, N. El-Kadry, S.A. Mahmoud, *Thin Solid Films* **269**, 117–120 (1995)
6. R. Zhou, Q. Zhang, J. Tian, D. Myers, M. Yin, G. Cao, *J. Phys. Chem. C* **117**, 26948–26956 (2013)
7. O.K. Echendu, F.B. Dejene, I.M. Dharmadasa, *J. Mater. Sci. Mater. Electron.* **28**, 18865–18872 (2017)
8. O.K. Echendu, I.M. Dharmadasa, *Mater. Chem. Phys.* **157**, 39–44 (2015)
9. L.L. Kazmerski, F.R. White, G.K. Morgan, *Appl. Phys. Lett.* **29**, 268–270 (1976)
10. I. Repins, M.A. Contreras, B. Egaas, C. DeHart, J. Scharf, C.L. Perkins, B. To, R. Noufi, *Prog. Photovolt. Res. Appl.* **16**, 235–239 (2008)
11. X. Wang, S.S. Li, C.H. Huang, S. Rawal, J.M. Howard, V. Craciun, T.J. Anderson, O.D. Crisalle, *Sol. Energy Mater. Sol. Cells* **88**, 65–73 (2005)
12. X. Wang, S.S. Li, W.K. Kim, S. Yoon, V. Craciun, J.M. Howard, S. Easwaran, O. Manasreh, O.D. Crisalle, T.J. Anderson, *Sol. Energy Mater. Sol. Cells* **90**, 2855–2866 (2006)
13. F. Liu, Y. Lai, J. Liu, B. Wang, S. Kuang, Z. Zhang, J. Li, Y. Liu, *J. Alloys Compd.* **436**, 305 (2010)
14. W.G.C. Kumara, V.A. L.B.D.R.P Wijesundara, C.P. Seneviratne, B.S. Jayalath, Dassanayake, *Procedia Eng.* **139**, 64 (2016)
15. O.K. Echendu, U.S. Mbamara, K.B. Okeoma, C. Iroegbu, C.A. Madu, I.C. Ndukwe, I.M. Dharmadasa, *J. Mater. Sci. Mater. Electron.* **27**, 10182 (2016)
16. N.A. Abdul-Manaf, A.R. Weerasinghe, O.K. Echendu, I.M. Dharmadasa, *J. Mater. Sci. Mater. Electron.* **26**, 2429 (2015)
17. P. Boieriu, R. Sporcken, A. Adriaens, Y. Xin, N.D. Browning, S. Sivananthan, *Nucl. Instrum. Methods Phys. Res. Sect. B Beam Interact. Mater. Atoms* **161–163**, 975 (2000)
18. E.W. Jones, V. Barrioz, S.J.C. Irvine, D. Lamb, *Thin Solid Films* **517**, 2226 (2009)
19. V. Krishnakumar, K. Ramamurthi, A. Klein, W. Jaegermann, *Thin Solid Films* **517**, 2558 (2009)
20. M. Saglam, A. Ates, B. Guzeldir, A. Astam, M.A. Yildirim, *J. Alloys Compd.* **484**, 570 (2009)
21. P.J. Sebastian, M.E. Calixto, Porous, *Thin Solid Films* **360**, 128–132 (2002)
22. A.A. Ziabari, F.E. Ghodsi, Growth, *Sol. Energy Mater. Sol. Cells* **105**, 249–262 (2012)
23. S. Bonilla, E.A. Dalchiale, *Thin Solid Films* **204**, 397 (1991)
24. B. Ullrich, H. Sakai, Y. Segawa, *Appl. Phys. Lett.* **80**, 356–358 (2002)
25. M. Rusu, T. Glatzel, A. Neisser, C.A. Kaufmann, S. Sadewasser, M.C. Lux-, Steiner, *Appl. Phys. Lett.* **88**, 143510 (2006)
26. I.M. Dharmadasa, O.K. Echendu, *Encycl. Appl. Electrochem.* (2012) 680–691
27. J. Nishino, S. Chatani, Y. Uotani, Y. Nosaka, *J. Electroanal. Chem.* **473**, 217–222 (1999)
28. G. Mustafa, M.R.I. Chowdhury, D.K. Saha, S. Hussain, O. Islam, *Dhaka Univ. J. Sci.* **60**, 283 (2012)
29. V. Singh, P. Chauhan, *J. Phys. Chem.* **70**, 1074–1079 (2009)
30. K.G. Rao, V.K. Ashith, *J. Phys. Chem.* **77**, 14–22 (2015)
31. O. Zelaya-Angel, R. Lozada-Morales, *Phys. Rev. B* **62**, 13064 (2000)
32. L. Wenyi, C. Xun, C. Qiulong, Z. Zhibin, *Mater. Lett.* **59**, 1–5 (2005)
33. F. Liu, Y. Lai, J. Liu, B. Wang, S. Kuang, Z. Zhang, J. Li, Y. Liu, *J. Alloys Compd.* **493**, 305–308 (2010)
34. A. Mukherjee, B. Satpati, S.R. Bhattacharyya, R. Ghosh, P. Mitra, *Phys. E* **65**, 51–55 (2015)
35. M.J. Kim, H.T. Kim, J.K. Kang, D.H. Kim, D.H. Lee, S.H. Lee, S.H. Sohn, *Mol. Cryst. Liq. Cryst.* **532**, 21 (2010)
36. R.R.L. De Oliveira, D.A.C. Albuquerque, T.G.S. Cruz, F.M. Yamaji, F.L. Leite, <http://www.intechopen.com>. InTech (2012)
37. J. Aguilar-Hernandez, J. Saatre-Hernandez, N. Ximello-Quebras, R. Mendoza-, O. Perez, G. Vigil-Galan, Contreras-Garcia, *Thin Solid Films* **143**, 511–512 (2006)
38. K. Ravichandran, P. Philominathan, *Appl. Surf. Sci.* **255**, 5736–5741 (2009)